

Bandgap Change of Carbon Nanotubes: Effect of Small Uniaxial and Torsional Strain

Liu Yang¹, M. P. Anantram^{2*}, Jie Han² and J. P. Lu^{2a}

¹ *Thermosciences Institute, NASA Ames Research Center, Mail Stop 230-3, Moffett Field, CA, USA 94035-1000*

² *NASA Ames Research Center, Mail Stop T27A-1, Moffett Field, CA, USA 94035-1000*

Abstract

We use a simple picture based on the π electron approximation to study the bandgap variation of carbon nanotubes with uniaxial and torsional strain. We find (i) that the magnitude of slope of bandgap versus strain has an almost universal behaviour that depends on the chiral angle, (ii) that the sign of slope depends on the value of $(n - m) \bmod 3$ and (iii) a novel change in sign of the slope of bandgap versus uniaxial strain arising from a change in the value of the quantum number corresponding to the minimum bandgap. Four orbital calculations are also presented to show that the π orbital results are valid.

Typeset using REVTeX

I. INTRODUCTION

The mechanical and electronic properties of carbon nanotubes (CNT) have individually been studied in some detail¹⁻⁵ and the predicted dependence of bandgap on chirality¹⁻³ has been observed.⁶ The study of bandgap variation with mechanical deformation is important in view of the ability to manipulate individual nanotubes⁷. Additionally, they could form the basis for nanoscale sensors in a manner similar to experiments using C_{60} molecules.⁸ Recent studies of bandgap change of zigzag and armchair tubes on mechanical strain have shown interesting behavior.⁹⁻¹¹ Refs. 9 and 10 studied the effect of uniaxial strain using a Green's function method based on the π electron approximation and a four orbital numerical method, respectively. Ref. 11 predicted the opening of a bandgap in armchair tubes under torsion, using a method that wraps a massless two dimensional Dirac Hamiltonian on a curved surface. In this paper, we present a simple and unified picture of the band gap variation of chiral and achiral CNT with uniaxial and torsional strain. The method used is discussed in section II. The results obtained by using a single π orbital are discussed in section III A and are compared to four orbital calculations in section III B. The conclusions are presented in section IV.

II. METHOD

In the presence of a uniform uniaxial and torsional strain, a distorted graphene sheet continues to have two atoms per unit cell [Fig. 1]. It is convenient to represent the change in bond lengths using the chirality dependent coordinate system. The axes of the chirality dependent coordinate system corresponding to (n, m) CNT are the line joining the $(0, 0)$ and (n, m) carbon atoms (\hat{c}), and its perpendicular (\hat{t}) [Fig. 1].¹² The fixed and chirality dependent coordinate system are related by, $\hat{c} = \cos\theta\hat{x} + \sin\theta\hat{y}$ and $\hat{t} = -\sin\theta\hat{x} + \cos\theta\hat{y}$, where, $\sin(\theta) = \frac{1}{2} \frac{n-m}{c_h}$ and $\cos(\theta) = \frac{\sqrt{3}}{2} \frac{n+m}{c_h}$. $c_h = \sqrt{n^2 + m^2 + nm}$, is the circumference of the tube in units of the equilibrium lattice vector length, $|\vec{a}_1| = |\vec{a}_2| = a_0$. The bond vectors are given

by,

$$\vec{r}_1 = \frac{a_0}{2} \frac{n+m}{c_h} \hat{c} - \frac{a_0}{2\sqrt{3}} \frac{n-m}{c_h} \hat{t} + \delta\vec{r}_1 \text{ and } \vec{r}_2 = -\frac{a_0}{2} \frac{m}{c_h} \hat{c} + \frac{a_0}{2\sqrt{3}} \frac{2n+m}{c_h} \hat{t} + \delta\vec{r}_2, \quad (1)$$

where, $\delta\vec{r}_i$ represents deviation from an undistorted sheet and $\vec{r}_3 = -(\vec{r}_1 + \vec{r}_2)$. Within the context of continuum mechanics, application of a uniaxial or torsional strain causes the following change in the bond vectors of Fig. 1:

$$r_{it} \rightarrow (1 + \epsilon_t)r_{it} \text{ and } r_{ic} \rightarrow (1 + \epsilon_c)r_{ic} \text{ (tensile)} \quad (2)$$

$$r_{ic} \rightarrow r_{ic} + \tan(\gamma)r_{it} \text{ (torsion)}, \quad (3)$$

where, $i = 1, 2, 3$ and r_{ip} is the p-component of \vec{r}_i ($p = c, t$). ϵ_t and ϵ_c represent the strain along \hat{t} and \hat{c} respectively, in the case of uniaxial strain. γ is the shear strain.

Using Eqs. (1)-(3), the lattice vectors of the distorted sheet are,

$$\vec{a}_1 = \vec{r}_1 - \vec{r}_3 = a_0[(1 + \epsilon_c)\frac{1}{2}\frac{2n+m}{c_h} + \tan(\gamma)\frac{\sqrt{3}}{2}\frac{m}{c_h}]\hat{c} + a_0(1 + \epsilon_t)\frac{\sqrt{3}}{2}\frac{m}{c_h}\hat{t} \quad (4)$$

$$\vec{a}_2 = \vec{r}_1 - \vec{r}_2 = a_0[(1 + \epsilon_c)\frac{1}{2}\frac{n+2m}{c_h} - \tan(\gamma)\frac{\sqrt{3}}{2}\frac{n}{c_h}]\hat{c} - a_0(1 + \epsilon_t)\frac{\sqrt{3}}{2}\frac{n}{c_h}\hat{t}. \quad (5)$$

The corresponding unit cell area is $|\vec{a}_1 \times \vec{a}_2| = \frac{\sqrt{3}}{2}(1 + \epsilon_t)(1 + \epsilon_c)a_0^2$. The real space unit cells correspond to $\vec{r} = j_1\vec{a}_1 + j_2\vec{a}_2$, where j_1 and j_2 are integers. The 1D unit cell length (T) is the shortest r_t for which $r_c = 0$. That is, the two lattice points, $\vec{r} = 0$ and $\vec{r} = j_1\vec{a}_1 + j_2\vec{a}_2$ have the same \hat{c} coordinate. This corresponds to the following condition on j_i and j_2 ,

$$(1 + \epsilon_c)[j_1(2n + m) + j_2(n + 2m)] + \tan(\gamma)\sqrt{3}[j_1m - j_2n] = 0 \quad (6)$$

and the 1D unit cell length is,

$$T = a_0(1 + \epsilon_t)\frac{\sqrt{3}}{2}\frac{(j_1m - j_2n)}{c_h} \quad (7)$$

When only uniaxial strain is present ($\gamma = 0$), Eq. (6) corresponds to, $j_1(2n + m) + j_2(n + 2m) = 0$. The corresponding j_1 and j_2 with smallest absolute values are $j_1 = (n + 2m)/\gcd(2n + m, n + 2m)$ and $j_2 = -(2n + m)/\gcd(2n + m, n + 2m)$. \gcd refers to the

greatest common divisor. Using these values in Eq.(7), the 1D unit cell length of an (n,m) tube is,

$$T = (1 + \epsilon_t)\sqrt{3}c_h a_0 / \gcd(2n + m, n + 2m) . \quad (8)$$

In the absence of strain, Eq. (8) reduces to the result for undeformed nanotubes. In the presence of uniaxial strain, the unit cell length is equal to $(1 + \epsilon_t)$ times the unstrained unit cell length. When only torsion is present, Eq. (6) simplifies to,

$$j_1(2n + m) + j_2(n + 2m) + \tan(\gamma)\sqrt{3}(j_1m - j_2n) = 0 . \quad (9)$$

For arbitrary values of γ , n and m , this equation corresponds to a large T . For example, from Fig. 1 it is easy to see that under torsion, the unit cell of an armchair tube can be much larger than a_0 depending on the value of γ . We will come back to this point at the end of section II, where we discuss calculation of bandgap change due to torsion.

We treat the nanotube within the approximation that it is a rolled up graphene sheet and assume a single π orbital per carbon atom. We calculate the band structure of the distorted sheet to be,¹³

$$E(\vec{k}) = (t_1^2 + t_2^2 + t_3^2 + 2t_1t_2 \cos[\vec{k} \cdot (\vec{r}_1 - \vec{r}_2)] + 2t_2t_3 \cos[\vec{k} \cdot (\vec{r}_2 - \vec{r}_3)] + 2t_3t_1 \cos[\vec{k} \cdot (\vec{r}_3 - \vec{r}_1)])^{\frac{1}{2}} , \quad (10)$$

where, $\vec{k} = k_c\hat{c} + k_t\hat{t}$. The primary effects of change in bond vectors are to alter the hopping parameter between carbon atoms and lattice vectors. The hopping parameter is assumed to scale with bond length as,¹⁴ $t_i = t_0 (r_0/r_i)^2$, where t_0 and r_0 are the hopping parameter and bond length of an unstrained graphene sheet. The value of t_0 is around 3eV. From Eqs. (4) and (5), the circumference of the distorted sheet is $(1 + \epsilon_c)c_h a_0$. The wave function of the CNT is quantized around the circumference and so k_c is given by,

$$k_c(1 + \epsilon_c)c_h a_0 = 2\pi q , \quad (11)$$

where, q is an integer. Eq. (10) can now be written as,

$$\begin{aligned}
E(k_t) = & (t_1^2 + t_2^2 + t_3^2 + 2t_1t_2 \cos[\pi q \frac{n+2m}{c_h^2} - \frac{\sqrt{3}}{2} \frac{n}{c_h} k'_t a_0 - \pi q \frac{\sqrt{3} \tan(\gamma)}{1+\epsilon_c} \frac{n}{c_h^2}] \\
& + 2t_1t_3 \cos[\pi q \frac{2n+m}{c_h^2} + \frac{\sqrt{3}}{2} \frac{m}{c_h} k'_t a_0 + \pi q \frac{\sqrt{3} \tan(\gamma)}{1+\epsilon_c} \frac{m}{c_h^2}] \\
& + 2t_2t_3 \cos[\pi q \frac{n-m}{c_h^2} + \frac{\sqrt{3}}{2} \frac{n+m}{c_h} k'_t a_0 + \pi q \frac{\sqrt{3} \tan(\gamma)}{1+\epsilon_c} \frac{n+m}{c_h^2}])^{\frac{1}{2}}, \quad (12)
\end{aligned}$$

where, $k'_t = (1 + \epsilon_t)k_t$. The bandgap of an (n, m) tube in presence of uniaxial ($\gamma = 0$) or torsional strain ($\epsilon_c = \epsilon_t = 0$) can be easily calculated from Eq. (12). In case of uniaxial strain, the limits of k_t are given by $-\frac{\pi}{T} < k_t < \frac{\pi}{T}$, where T is the 1D lattice vector length determined by Eq. (8). The number of atoms in the 1D unit cell does not change in the presence of uniaxial strain and so the range of q does not change from the undeformed case ($q = 0, 1, 2, \dots, N_c$, where N_c is the number of hexagons in the 1D unit cell).

In the case of torsion, the number of atoms in the 1D unit cell and T can be large [Eq. (9)]. The corresponding span of k_t is then small compared to the undeformed tube and the range of q is commensurate with the number of atoms in the 1D unit cell. The eigen spectrum can however be obtained from Eq. (12) by setting $\gamma = 0$ and spanning over the same values of q and k_t as in the undeformed case. This is because the eigen spectrum depends only on the tight binding parameters (and not on the exact geometry) if the coordination number of the carbon atoms remains constant.¹⁵

III. RESULTS AND DISCUSSION

The results obtained using the method described in section II are discussed in section III A. We then present the results from four orbital calculations with energy minimized structures in section III B.

A. π orbital

We first consider the case of uniaxial strain. The bandgap is obtained by finding the minimum of $E(k_t)$, where the span of k_t and q are discussed below Eq. (12). The bandgap

change is largest for zigzag tubes and the magnitude of $|dE_g/d\sigma|$ is approximately equal to $3t_0$. For armchair tubes, application of uniaxial strain does not cause a bandgap. We find that, (i) $|dE_g/d\sigma|$ increases with increase in chiral angle [Fig. 2] and (ii) the sign of $dE_g/d\sigma$ follows the $(n - m) \bmod 3$ rule.¹⁶ For example, the chiral angle of (6, 5) and (6, 4) tubes are close to that of armchair tubes. The slope of bandgap versus strain is correspondingly small and the sign of slope are opposite. For semiconducting zigzag tubes and armchair tubes, our results agree with Ref. 9.

As uniaxial strain increases, there is an abrupt reversal in sign of $dE_g/d\sigma$ as illustrated for zigzag tubes in Fig. 4. This feature indicates a change in band index q corresponding to the bandgap and can be understood from the following expression that describes dependence of energy for various values of q at $k_t = 0$ [Eq. (16) of appendix]:

$$E(0) = E_0(q) - 2t_0 \frac{\delta r_1}{r_0} \left[1 - \frac{2\delta r_2}{\delta r_1} \cos\left(\frac{q\pi}{n}\right) \right] \text{sgn}(x), \quad (13)$$

where, $\text{sgn}(x) = [1 - 2\cos(q\pi/n)]$. The minimum value of $E_0(q) = t_0 |1 - 2\cos(q\pi/n)|$ is half of the bandgap of an unstrained tube. The first term of Eq. (13) takes the smallest value for the band index $q = q_0$ that satisfies $n = 3q_0 \pm 1$. The second term can however change sign when q changes from q_0 to $q_0 \pm 1$. As a result, a dramatic change in sign of $dE_g/d\sigma$ becomes possible if the magnitude of the second term is larger than change in the first term [Fig. 3]. The strain required to observe this effect decreases as the inverse radius of tube for large n . This is because the difference in energy of the q_0 and $q_0 \pm 1$ bands become smaller with increase in radius. Fig. 3 demonstrates this point by comparing the (10,0) and (19,0) tubes. For the (19,0) tube, the change in slope occurs at around five percent strain. These strain values are accessible in bulk nanotube samples.¹⁷ The inset of Fig. 3 shows change in energy of the $q=6$ and $q=7$ bands for the (19,0) tube for three different values of strain. While the $q=6$ band shifts up in energy as strain increases, the $q=7$ band shifts down. Thus leading to the discussed change in sign of $dE_g/d\sigma$.

In case of torsional strain, the bandgap is obtained by finding the minimum of $E(k_t)$ using Eq. (12), where the span of k_t and q are discussed in the last paragraph of section II.

The magnitude of $|dE_g/d\sigma|$ is approximately equal to $3t_0$ for armchair tubes and this is in agreement with Ref. 11. For zigzag tubes, torsion causes only a small change in bandgap. The leading term in bandgap change depends on γ only to second order. We find that, (i) $|dE_g/d\sigma|$ decreases with increase in chiral angle and takes the smallest value for zigzag tubes [Fig. 4] and (ii) the sign of $dE_g/d\sigma$ follows the $(n - m) \bmod 3$ rule.¹⁶

B. Four orbital

To verify the simple picture presented, we have also performed four orbital calculations using the parametrization given in Ref. 18. The change in bond lengths are computed using both continuum mechanics [Eqs. (2) and (3)] and structures that are energy minimized by Brenner potential.¹⁹ The energy minimization was performed with periodic boundary conditions. For the small values of strain considered, we find that the bandgap is not very sensitive to the two methods of obtaining the bond lengths. The results presented in Figs. 5 and 6 correspond to the bond lengths obtained by energy minimization. For semiconducting tubes, the results of Figs. 5 and 6 agree with the π orbital results presented in Figs. 2 and 4 respectively: The slope of $dE_g/d\sigma$ follows the $(n - m) \bmod 3$ rule and the magnitude of slope varies monotonically with chiral angle. The primary difference concerns non armchair tubes satisfying $n - m = 3 * integer$. This is not surprising because Ref. 2 has predicted such tubes to have a small bandgap due to curvature induced hybridization at zero strain. As a result, applying either tension or compression does not produce the "V" shaped curve of Fig. 2 with zero bandgap at zero strain. The difference is that the curves are shifted away from the origin as shown in Fig. 5.

IV. CONCLUSIONS

In conclusion, we present a simple picture to calculate bandgap versus strain of CNT with arbitrary chirality. We find that under uniaxial strain, $|dE_g/d\sigma|$ of zigzag tubes is $3t_0$ independent of diameter, and continually decreases as the chirality changes to armchair,

when it takes the value zero. In contrast, we show that under torsional strain, $|dE_g/d\sigma|$ of armchair tubes is $3t_0$ independent of diameter, and continually decreases as the chirality changes to zigzag, where it takes a small value. The sign of $dE_g/d\sigma$ follows the $(n-m) \bmod 3$ rule in both cases.¹⁶ We also predict a change in the sign of $dE_g/d\sigma$ as a function of strain, corresponding to a change in the value of q that corresponds to the bandgap minimum. Comparison to four orbital calculations show that the main conclusions are unchanged. The primary difference involves nonarmchair tubes that satisfy $n - m = 3 * integer$.

This work is supported by NASA contracts NAS2-14031 to Elore (LY), NASA Ames Research Center and U.S. Department of Energy (JPL).

V. APPENDIX

Zigzag tubes under tension: Under uniaxial strain the band structure of $(n, 0)$ is,

$$E(k_t) = \pm t_2 \left[1 \pm \left(\frac{4t_1}{t_2} \right) \cos\left(\frac{q\pi}{n}\right) \cos\left((1 + \epsilon_t) \frac{\sqrt{3}}{2} k_t a_0\right) + \left(\frac{2t_1}{t_2} \right)^2 \cos^2\left(\frac{q\pi}{n}\right) \right]^{\frac{1}{2}}. \quad (14)$$

$t_1 = t_3$ due to symmetry. The minimum of $E(k_t)$ occurs at $k_t = 0$,

$$E(0) = \pm t_2 \left| 1 - \frac{2t_1}{t_2} \cos\left(\frac{q\pi}{n}\right) \right|. \quad (15)$$

To first order in δr_i Eqn. (15) is,²⁰

$$E(0) = E_0(q) - 2t_0 \frac{\delta r_1}{r_0} \left[1 - \frac{2\delta r_2}{\delta r_1} \cos\left(\frac{q\pi}{n}\right) \right] \text{sgn}(x) \left[1 - 2\cos\left(\frac{q\pi}{n}\right) \right], \quad (16)$$

where, $\text{sgn}(x) = [1 - 2\cos(q\pi/n)]$ and $E_0(q) = t_0 |1 - 2\cos(q\pi/n)|$.

REFERENCES

- * anant@nas.nasa.gov; Corresponding author
- ^a Permanent address: CB 3255 Phillips Hall, University of North Carolina - Chapel Hill, Chapel Hill, NC 27599;
- ¹ J. W. Mintmire, B. I. Dunlap and C. T. White, Phys. Rev. Lett. **68**, 631 (1992);
- ² N. Hamada, S. Sawada and A. Oshiyama, Phys. Rev. Lett. **68**, 1579 (1992);
- ³ R. Saito, M. Fujita, G. Dresselhaus and M. S. Dresselhaus, Appl. Phys. Lett. **60**, 2204 (1992)
- ⁴ M. S. Dresselhaus, G. Dresselhaus and P. C. Eklund, Chap. 19 of Science of Fullerenes and Carbon Nanotubes, Academic Press, (1996)
- ⁵ B. I. Yakobson, App. Phys. Lett. **72**, 918 (1998); M. B. Nardelli, B. I. Yakobson, J. Bernholc Phys. Rev. B **57** 4277 (1998)
- ⁶ J. W. G. Wildoer, L. C. Venema, A. G. Rinzler, R. E. Smalley and C. Dekker, Nature **391**, 59 (1998) and T. W. Odom, J. L. Huang, P. Kim and C. M. Lieber, Nature **391**, 62 (1998)
- ⁷ L. C. Venema, J. W. G. Wildoer, H. L. J. T. Tuinstra, C. Dekker, A. G. Rinzler and R. E. Smalley Appl. Phys. Lett. **71**, 2629 (1997)
- ⁸ C. Joachim, J. K. Gimzewski, R. R. Schlittler, and C. Chavy, Phys. Rev. Lett. **74**, 2102 (1995)
- ⁹ R. Heyd, A. Charlier, E. McRae, Phys. Rev. B **55**, 6820 (1997).
- ¹⁰ D. W. Brenner, Private Communication.
- ¹¹ C. L. Kane and E. J. Mele, Phys. Rev. Lett **78**, 1932 (1997)
- ¹² C. T. White, D. H. Robertson and J. W. Mintmire, Phys. Rev. B **47**, 5485 (1993); D. J.

Klein, W. A. Seitz and T. G. Schmalz, J. Phys. Chem. **97**, 1231 (1993); P. J. Lin-Chung and A. K. Rajagopal, J. Phys.: Condens. Matter **6**, 3697 (1994)

¹³ This expression can be obtained by extending the treatment of P. R. Wallace, Phys. Rev. **71**, 622 (1947) to the case of a graphene sheet with three bonds with unequal bond lengths and hopping parameters.

¹⁴ W. A. Harrison, Electronic structure and the properties of solids, Dover Publication Inc., New York (1989)

¹⁵ This discussion applies to the tensile case also, where ϵ_t and ϵ_c should be set equal to zero. At the end of the last paragraph we however did not use this argument to generate the eigen spectrum because the 1D unit cell length simply scales as $(1 + \epsilon_t)$. The essence of this discussion is that if the change in hopping parameters is accounted for, then the eigen spectrum can be calculated by assuming that the geometry has not changed.

¹⁶ defined in terms of $\{-1, 0, 1\}$; i.e., $(n - m) \bmod 3$ equal to 0, 1 and 2 corresponds to 0, 1, and -1 respectively in the notation used.

¹⁷ D. A. Walters, L. E. Ericson, M. J. Casavant, J. Liu, D. T. Colbert and R. E. Smalley, "The Elastic Limit of Single-Wall Nanotube Ropes"; T. Rueckes, C. L. Cheung, J. W. Hutchinson and C. M. Lieber, "Tensile Strength of Carbon Nanotubes". Both references are in 1999 centennial meeting bulletin of the American Physical Society, Vol.44, No.1, Part II (1999), page 1818, Centennial Meeting, American Physical, March 20-26, 1999, Atlanta, Georgia

¹⁸ D. Tomanek and S. G. Louie, Phys. Rev. B **37**, 8327 (1988).

¹⁹ D. W. Brenner Phys. Rev. B **42**, 9458 (1990)

²⁰ $2t_0\delta r_i$ can be replaced by δt_i in this expression.

Figure Captions:

Fig. 1: The fixed (x, y) and chirality dependent (\hat{c}, \hat{t}) coordinates. r_1 , r_2 and r_3 correspond to bonds 1, 2 and 3 respectively. \vec{a}_1 and \vec{a}_2 are the lattice vectors of the two dimensional sheet.

Fig. 2: Bandgap versus tensile strain: For semiconducting tubes, the sign of slope of $d(Bandgap)/d(Strain)$ depends only on the value of $(n - m) \bmod 3$. The magnitude of $d(Bandgap)/d(Strain)$ is largest for zigzag tubes and decreases with decrease in chiral angle. The magnitude is smallest for armchair tubes. The solid, dashed and dotted lines correspond to $(n - m) \bmod 3$ values of 1, -1 and 0 respectively. The value of t_0 is around 3eV.

Fig. 3: The change in slope of the (10,0) and (19,0) tubes around 10% and 5% strain respectively is due to a change in the quantum number q that yields the minimum bandgap. Inset: E vs k of the $q=7$ (solid) and $q=6$ (dashed) bands as a function of strain for a (19,0) tube. Strains of 0%, 3% and 6% correspond to increasing thickness of the lines.

Fig. 4: Bandgap versus torsional strain: For semiconducting tubes, the sign of slope of $d(Bandgap)/d(Strain)$ depends only on the value of $(n - m) \bmod 3$. The magnitude of $d(Bandgap)/d(Strain)$ is largest for armchair tubes and decreases with increase in chiral angle. The magnitude is smallest for zigzag tubes. The solid, dashed and dotted lines correspond to $(n - m) \bmod 3$ values of 1, -1 and 0 respectively.

Fig. 5: Same as Fig. 2 with the only difference that these are four orbital results. In the y-axis label, $t=2.66\text{eV}$.

Fig. 6: Same as Fig. 4 with the only difference that these are four orbital results. In the y-axis label, $t=2.66\text{eV}$.

FIGURES

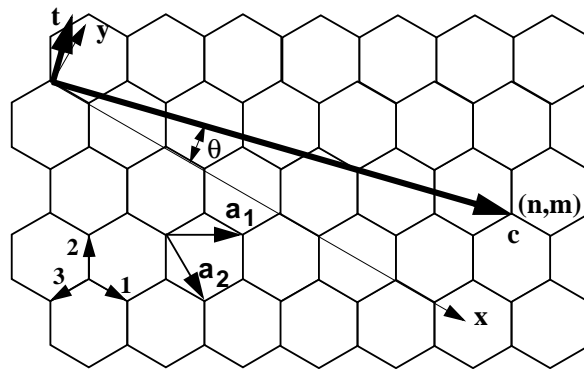


Fig. 1 / Yang

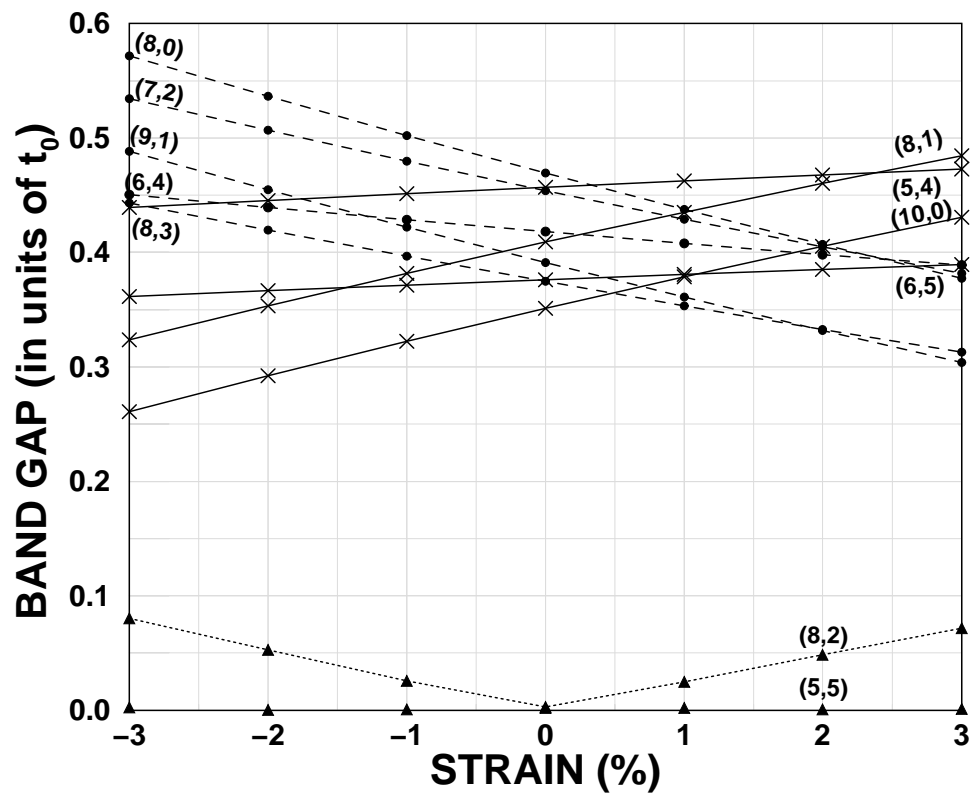
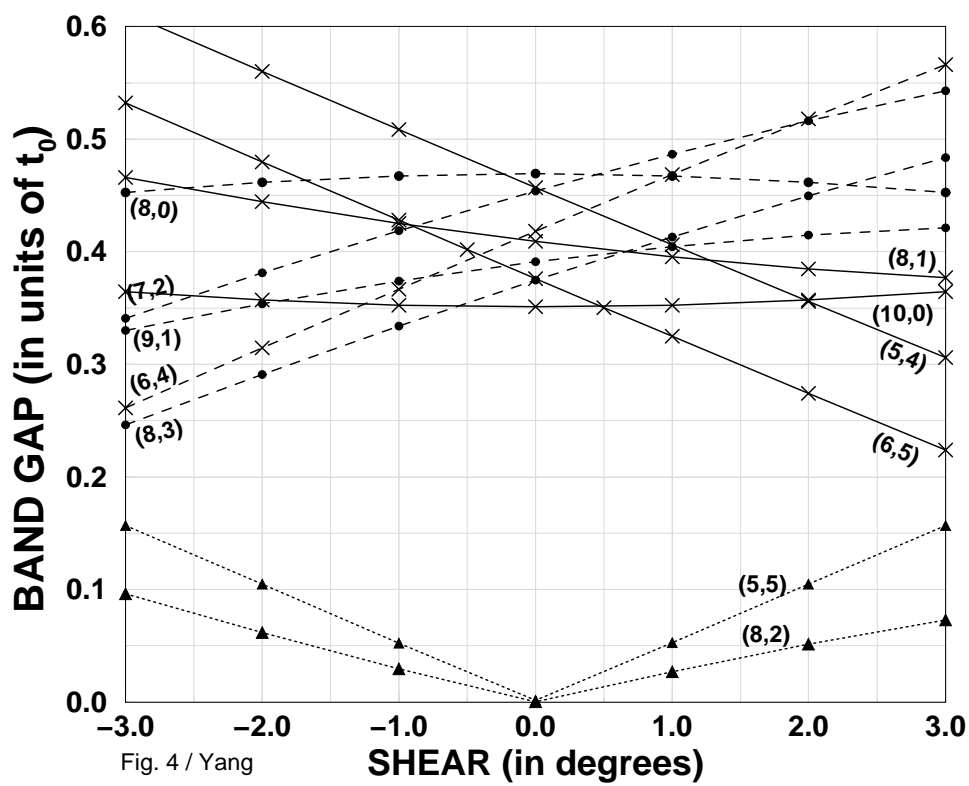
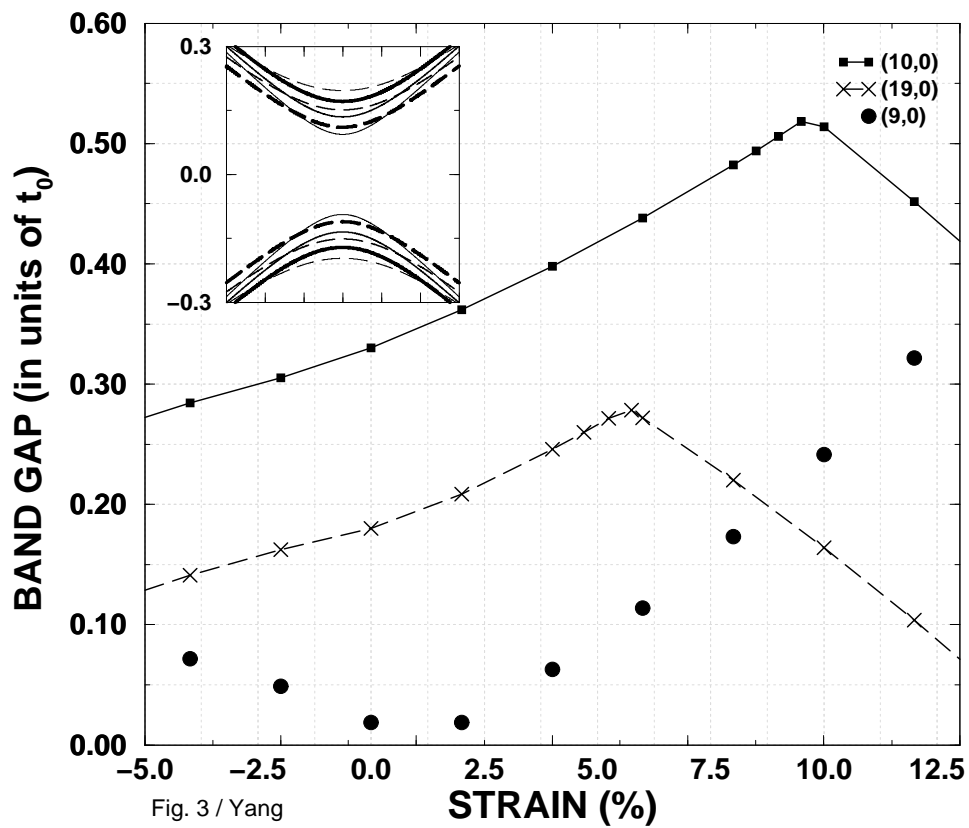


Fig. 2 / Yang



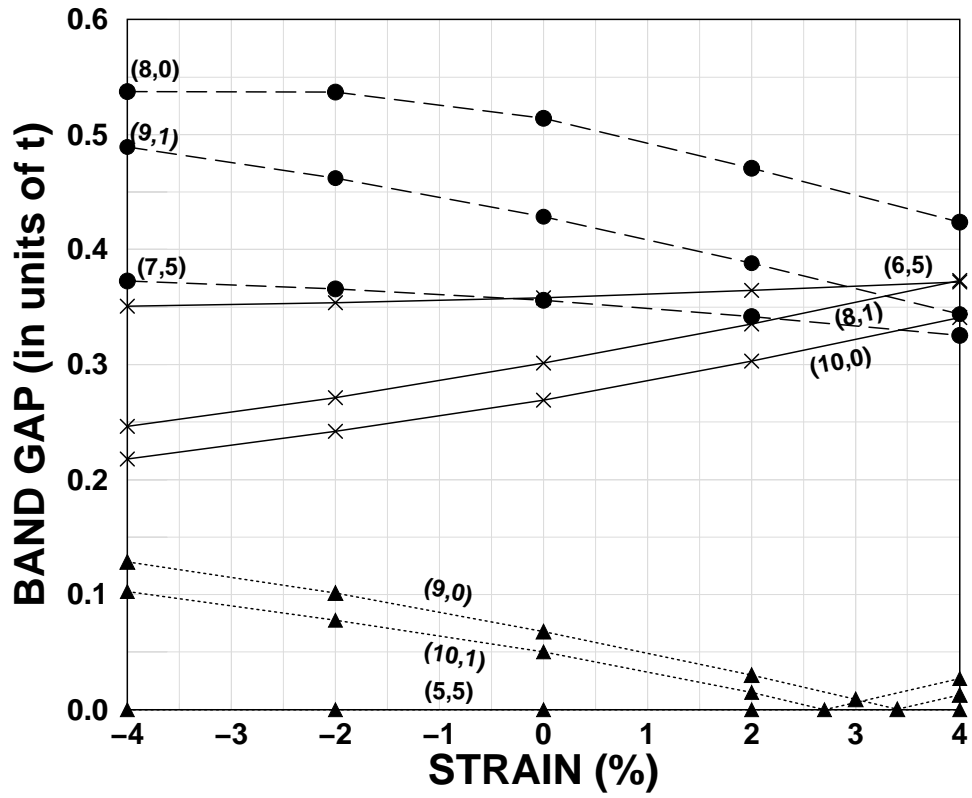


Fig. 5 / Yang

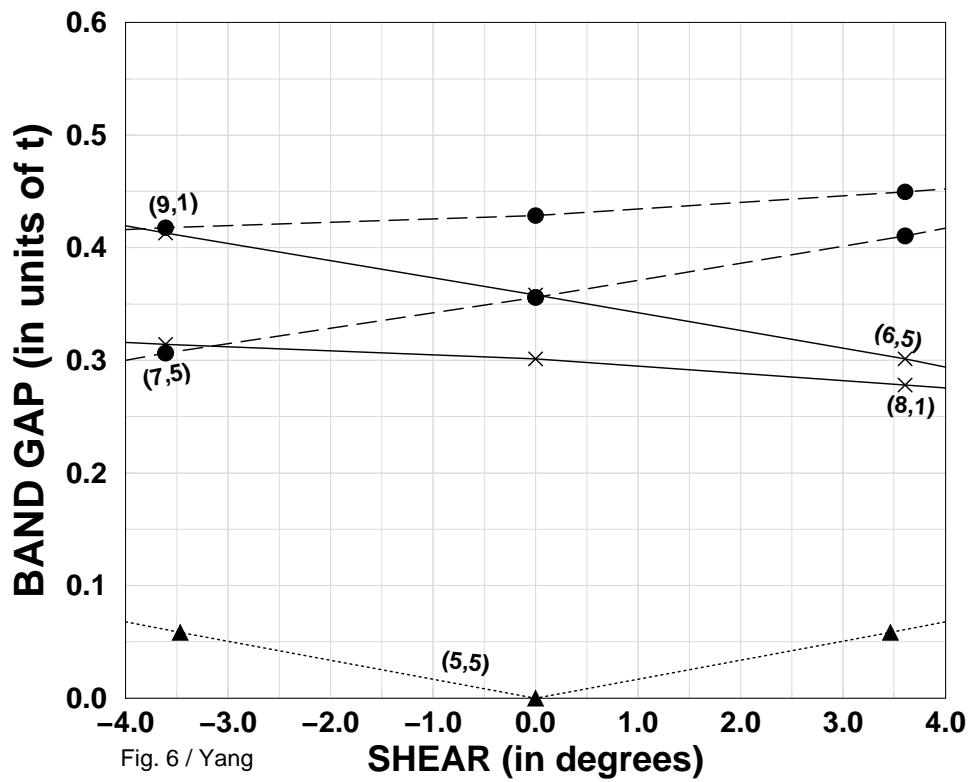


Fig. 6 / Yang